Theoretical Study of Structural and Electronic Properties of H-Silsesquioxanes

Kai-Hua Xiang,[†] Ravindra Pandey,*[,†] Udo C. Pernisz,[‡] and Clive Freeman[§]

Department of Physics, Michigan Technological University, Houghton, Michigan 49931, Dow Corning Corporation, Midland, Michigan 48686, and Molecular Simulations Inc., San Diego, California 92121

Received: April 14, 1998; In Final Form: August 19, 1998

The results of first principles calculations on H-silsesquioxanes (i.e., $(HSiO_{3/2})_n$ with $n = 4$, 6, 8, 10, 12, 14, and 16) are reported here. Double numeric basis sets and local and nonlocal density approximations to density functional theory are employed for calculations. It is shown that use of the nonlocal density approximation is required for the reliable prediction of the most stable isomer for silsesquioxanes. Furthermore, a progression of the preferred building unit with the increase in size of the T cage is revealed. The smaller T cages prefer four- and five-member rings while the larger cages are found to prefer four- and six-member rings. Analysis of the energy of the hydrolysis reaction, binding energy, and fragmentation paths finds the relative stability of the silsesquioxane cages containing four-, five-, and six-member rings in agreement with experimental observations. For the $(HSiO_{3/2})_{16}$ cage, the calculated results predict the stability of the D_{2d}-$6^4 5^0 4^6$ configuration over the D_{4d}-$6^0 5^8 4^2$ configuration in contradiction to suggestions based on ^{29}Si NMR measurements. We find a consistent picture for the highest occupied molecular orbitals (HOMOs) of all silsesquioxanes considered showing them to be composed of (lone-pair) oxygen p-type atomic orbitals. On the other hand, the lowest unoccupied molecular orbitals (LUMOs) show size dependence in their composition which appears to cause the presence of a state in the HOMO−LUMO gap for higher silsesquioxane cages. Density of states plots and analysis of molecular orbitals reveal this state to be due to the terminal hydrogens bonded to silicon atoms.

1. Introduction

H-silsesquioxanes (HSQ) constitute an important class of resinous inorganic polymers.[1−4] Their building block is the trifunctional monomer ($HSiO_{3/2}$), designated as the T unit. The structure of the polymer is based on siloxane-containing cages that are formed from the building block unit. For example, the T_8 structure forms a cage consisting of 8 silicon atoms that are connected by oxygen atoms to each other, whereas the T_{16} structure has a cage comprising 16 silicon atoms (Figures 1 and 2). The cross-linking of various siloxane-containing cages leads to a wide range in the distribution of molecular masses up to 200 kDa for the polymer. The cagelike structure of smaller T cages can also be considered as a building block for zeolite and silicate frameworks. For example, ring-opening vibrations of T cages were considered recently as a model system for the pore-opening vibrations of zeolites.[5−7]

The HSQ polymer is soluble in organic solvents, and the solution can be spin-cast to give thin films of HSQ that can be converted to low-density silica by heating in oxygen. As it is heated, the material undergoes a phase transition at approximately 200 °C during which it softens and flows. The film will not melt again after it has been converted. Therefore, gap fill and planarization on electronic circuits can be achieved by low-temperature processing of the polymer in a suitable atmosphere which enables the application of these films in the semiconductor industry for the manufacture of integrated circuits.[8] It was also observed that thin films of HSQ sandwiched between metal electrodes can exhibit bistability of the electric current−voltage characteristics in an inert atmosphere.[9] Under these circumstances, the current through the device is higher by several orders of magnitude than the insulating state, a reversible phenomenon that requires the presence of electronic states which facilitates the charge carrier transport in the material.

Although the synthesis of silsesquioxanes $(HSiO_{3/2})_n$ with $n = 8$, 10, 12, 14, and 16 has been reported,[2−14] there is a lack of information about electronic properties of silsesquioxanes, and the task of measuring and understanding these properties has become increasingly important for its technical application. In this paper, we perform such a task with two objectives: (i) determination of the ground-state configurations of the T_n cages with $n = 4$, 6, 8, 10, 12, 14, and 16 and (ii) prediction of the variation in electronic properties with the increase in cage size. We will consider various configurations of a given T cage and will perform total energy calculations to optimize its structural parameters, such as bond lengths and bond angles. For the optimized configurations, a trend in electronic properties will then be obtained by the analysis of molecular orbital energies and coefficients, electronic density maps, and density of states plots. In section 2, details of the computational techniques employed in this study are given. The results are presented and discussed in relation to experiments and previous calculations on the basis of the Hartree−Fock approximation in section 3. We give a summary and conclusions of this study in section 4.

2. Methods

All electron calculations on the T_n cages were performed in the framework of density functional theory using the program

[†] Michigan Technological University.
[‡] Dow Corning Corporation.
[§] Molecular Simulations Inc.

10.1021/jp981840r CCC: $15.00
Published on Web 10/06/1998

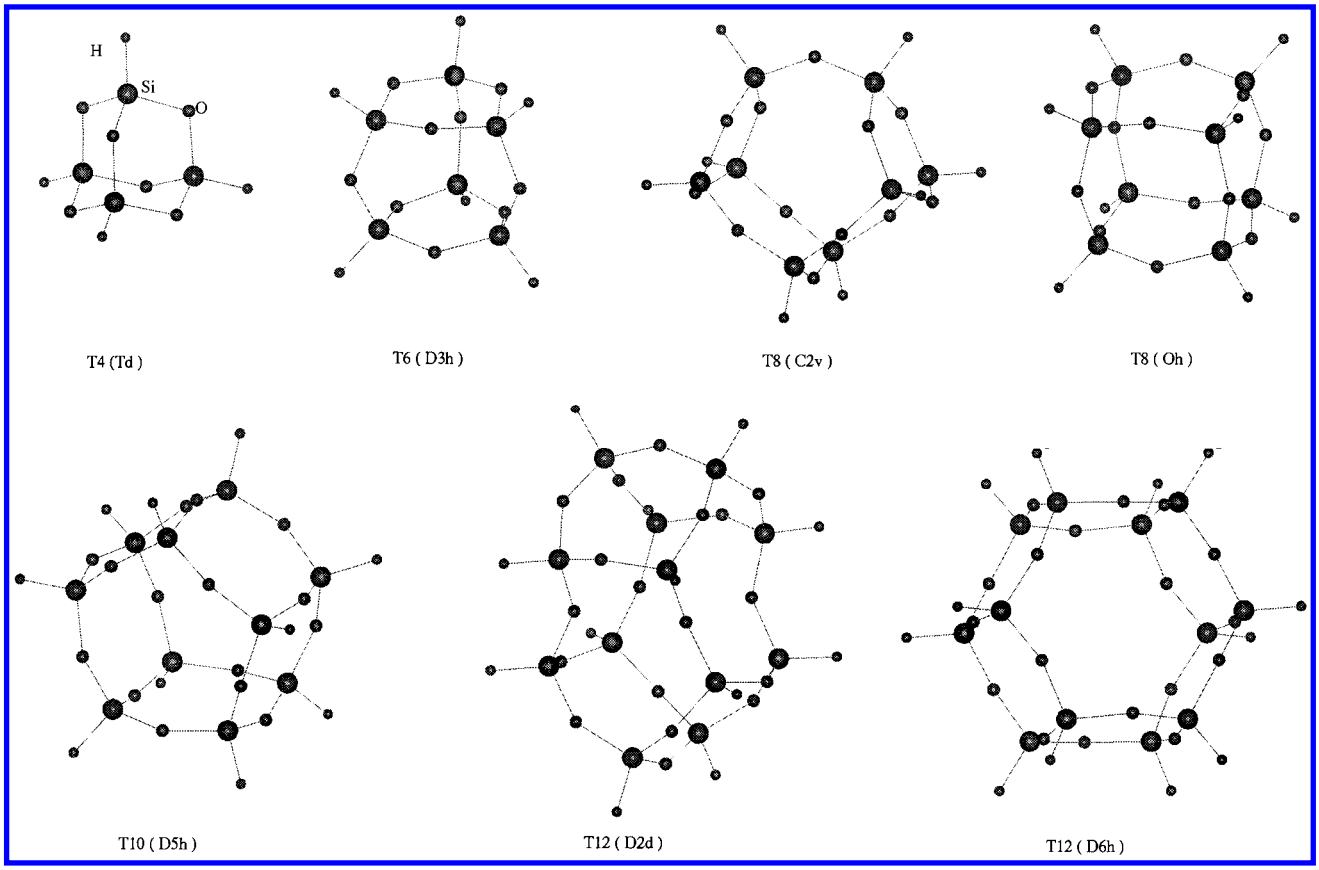

Figure 1. Optimized configurations of T_4, T_6, T_8, T_{10}, and T_{12} obtained in the nonlocal density approximation.

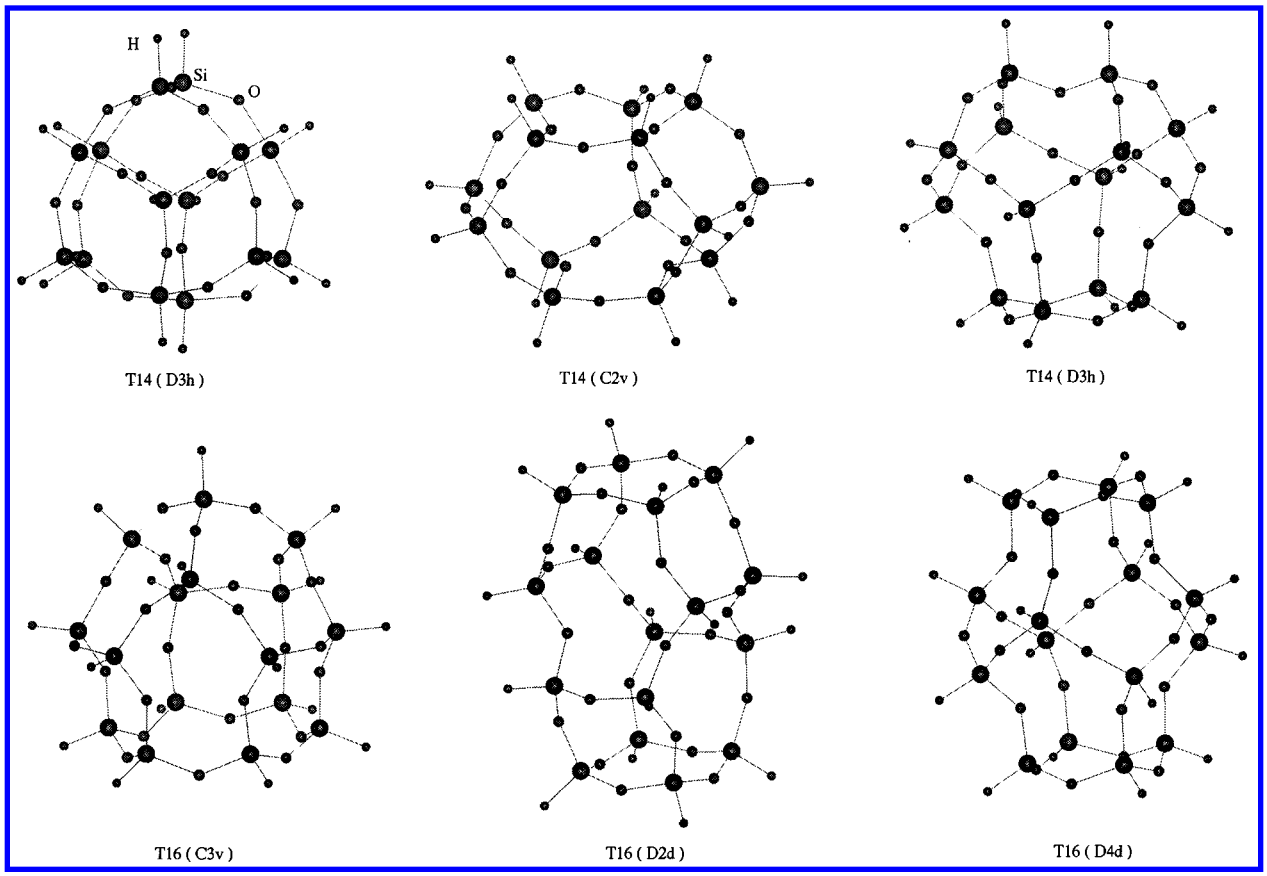

Figure 2. Optimized configurations of T_{14} and T_{16} obtained in the nonlocal density approximation.

package DMol.[15] We considered both local and nonlocal spin density approximations for the calculations. The Vosko−Wilk−Nusair local exchange and correlation functional[16] was used for the local density approximation (LDA) whereas a combination

TABLE 1: Total Energies for Various Configurations of Silsesquioxane Cages

				total energy (hartrees)			relative energy/Si atom (kcal/mol)		
	building unit	sym	state	LDA	NLDA	HF[22]	LDA	NLDA	HF[23]
T_4 ($H_4Si_4O_6$)	$5^0 4^0 3^4$	T_d	T_1	−1604.8263	−1616.1841	−1607.762	0	0	0
T_6 ($H_6Si_6O_9$)	$5^0 4^3 3^2$	D_{3h}	E′	−2407.2967	−2424.3336	−2411.716	−5.9	−6.0	−7.6
T_8 ($H_8Si_8O_{12}$)	$6^0 5^0 4^6$	O_h	A_{2g}	−3209.7425	−3232.4608	−3215.652	−7.0	−7.3	−10.0
	$5^2 4^2 3^2$	C_{2v}	B_1	−3209.7383	−3232.4534	−3215.639	−6.7	−6.7	−8.9
T_{10} ($H_{10}Si_{10}O_{15}$)	$6^0 5^2 4^5$	D_{5h}	E_2'	−4012.1756	−4040.5737	−4019.571	−6.9	−7.1	−10.3
T_{12} ($H_{12}Si_{12}O_{18}$)	$6^0 5^4 4^4$	D_{2d}	E	−4814.6188	−4848.6856	−4823.489	−7.3	−7.0	−10.5
	$6^2 5^0 4^6$	D_{6h}	B_{2u}	−4814.6085	−4848.6846	−4823.485	−6.8	−6.9	−10.3
T_{14} ($H_{14}Si_{14}O_{21}$)	$6^0 5^6 4^3$	D_{3h}	A_1''	−5617.0518	−5656.8071		−7.2	−7.3	
	$6^1 5^4 4^4$	C_{2v}	A_2	−5617.0581	−5656.8048		−7.4	−7.2	
	$6^3 5^0 4^6$	D_{3h}	A_1''	−5616.6062	−5656.2325		+12.8	+18.4	
T_{16} ($H_{16}Si_{16}O_{24}$)	$6^0 5^8 4^2$	D_{4d}	A_2	−6419.4636	−6464.9061		−6.2	−6.6	
	$6^1 5^6 4^3$	C_{3v}	E	−6419.4868	−6464.8917		−7.1	−6.1	
	$6^4 5^0 4^6$	D_{2d}	B_2	−6419.4834	−6464.9273		−7.0	−7.5	

TABLE 2: Selected Bond Lengths and Bond Angles of Silsesquioxanes[a]

			R_{Si-O} (pm)		A_{SiOSi} (deg)		A_{OSiO} (deg)	
	building unit	NR/N′R	LDA	NLDA	LDA	NLDA	LDA	NLDA
T_4	$5^0 4^0 3^4$ (T_d)	3R/3R	167	171	114.8	114.1	106.7	107.1
T_6	$5^0 4^3 3^2$ (D_{3h})	3R/4R	165	169	130.0	129.1		
		4R/4R	165	168	130.9	129.8	110.2	110.6
T_8	$6^0 5^0 4^6$ (O_h)	4R/4R	164	168	146.5	144.6	110.4	111.3
	$5^2 4^2 3^2$ (C_{2v})	3R/4R	165	169	130.2	126.4		
		3R/5R	165	169	130.4	128.9		
		4R/4R	163	168	179.1	146.2	109.8	110.7
		4R/5R	164	168	136.0	147.2		
		5R/5R	163	167	142.0	139.0	110.4	110.6
T_{10}	$6^0 5^2 4^5$ (D_{5h})	4R/4R	164	167	174.6	153.3	110.4	111.7
		4R/5R	164	167	140.5	149.0		
T_{12}	$6^0 5^4 4^4$ (D_{2d})	4R/4R	164	168	150.4	147.5	110.6	111.4
		4R/5R	164	168	140.2, 144.8	136.7, 145.0		
		5R/5R	164	168	143.6	143.8	108.8	109.9
	$6^2 5^0 4^6$ (D_{6h})	4R/4R	163	167	164.1	162.8	111.5	112.7
		4R/6R	163	167	145.0	143.3		
T_{14}	$6^0 5^6 4^3$ (D_{3h})	4R/5R	163	167	142.8	140.7		
		5R/5R	163	166	136.3, 174.6	141.4, 168.7	109.5	109.0
	$6^1 5^4 4^4$ (C_{2v})	4R/4R	164	168	158.2	158.6	110.9	111.7
		4R/5R	164	168	141.4, 146.1	141.3,141.8		
		4R/6R	164	168	143.9	140.1		
		5R/5R	164	167	130.2,140.0	139.8,141.1	109.3	109.7
		5R/6R	163	168	140.0	139.6		
	$6^3 5^0 4^6$ (D_{3h})	4R/4R	161	163	119.9	122.5		
		4R/6R	170	176	124.0	126.2		
		6R/6R	170	175	168.8	174.9		
T_{16}	$6^0 5^8 4^2$ (D_{4d})	4R/5R	164	168	154.9	134.2		
		5R/5R	163	168	174.3,175.7	137.9,150.5	110.2	110.0
	$6^1 5^6 4^3$ (C_{3v})	4R/5R	164	167	135.2, 146.1	131.8,145.0		
		4R/6R	164	167	146.7	144.7		
		5R/5R	163	167	156.7, 160.1	154.4,155.3	109.2	109.8
		5R/6R	164	168	138.1	134.5		
	$6^4 5^0 4^6$ (D_{2d})	4R/4R	164	168	149.3	147.8	112.3	112.1
		4R/6R	164	167	147.7,151.7,154.9	140.1,144.8,146.4		
		6R/6R	162	167	157.2	133.5	108.3	108.7

[a] The *N*R/*N*′R refers to the edge shared by *N*-member and *N*′-member (Si−O-) rings. The bond length R_{Si-H} is about 147 pm in both LDA and NLDA calculations.

of the gradient-corrected exchange functional of Becke[17] with the Vosko−Wilk−Nusair correlation functional was used for the nonlocal density approximation (NLDA). The double numeric basis sets,[18] supplemented by diffuse and polarization functions, were employed for H, Si, and O atoms. The accuracy of these basis sets has been analyzed in detail by Delley,[19] and such basis sets were recently used successfully to study structural and electronic properties of oxide clusters.[20,21] Since calculations proposed in this work are computationally intensive (e.g., the largest cluster considered here consists of 56 atoms with 432 electrons), we used the frozen-core approximation to reduce the computational cost. In this approximation, the $1s^2$ core orbital is frozen for oxygen and the $1s^2$ and $2s^2$ core orbitals are frozen for silicon during total energy calculations. We note that our earlier work has found negligible effects of freezing the core orbitals on the bond length, dissociation energy, and vibrational frequency in oxide clusters.[21] In the present calculations, the density tolerance was set to 10^{-6} au. The geometric parameters were fully optimized under the given symmetry group with a convergence criterion of both energy tolerance and maximum gradient component to be less than 10^{-5} hartree and 10^{-3} au, respectively. We have not performed frequency calculations on these clusters but note that similar parameters have proven successful in the study of a range of structural properties (see for example ref 21) for complex systems. The reliability of the numerical basis set can also be checked by

comparison of the calculated structural parameters for the T_8 cage with experiment[12] and previous electronic structure calculations.[22−24] The experimental values obtained from X-ray diffraction measurements for R_{Si-O}, A_{OSiO}, and A_{SiOSi} are 161.9 pm, 109.6°, and 147.5° respectively.

Calculations[22] based on the local density approximation using pseudopotentials report $R_{Si-O} = 162$ pm and $A_{SiOSi} = 148.6°$ while our LDA calculations using the numerical basis set find $R_{Si-O} = 164$ pm, $A_{OSiO} = 110.4°$, and $A_{SiOSi} = 146.5°$. On the other hand, the Hartree−Fock calculations[23] using the 6-31G-(d) basis set yield $R_{Si-O} = 163$ pm, $A_{OSiO} = 109°$, and $A_{SiOSi} = 149°$. Using a double-ζ plus polarization basis set for H and Si and a triple-ζ plus polarization basis set for O, Hill and Sauer[24] report $R_{Si-O} = 162.6$ pm and $A_{SiOSi} = 150°$. On the basis of this comparison, we therefore find that the double numerical basis set employed here appears to be very well suited for electronic structure calculations of H-silsesquioxanes.

It has been suggested that the molecular connectivity of various T cages can be described by 3-valent 3-connected convex polyhedra in which the vertexes represent the Si−H group and the edges represent the Si−O−Si linkage.[1−4] Following Agaskar and Klemperer,[3] we use the notation of N^n to represent n N-member rings. For example, the T_{14} cage may have isomeric configurations given by $6^05^64^3$ (six five-member and three four-member rings), $6^15^44^4$ (one six-member, four five-member, and four four-member rings), $6^25^24^6$ (two six-member, two five-member, and six four-member rings), and $6^35^04^6$ (three six-member and six four-member rings). For calculations, we do not consider all of the possible isomers of a T cage but restrict ourselves to those isomers identified by X-ray diffraction and NMR measurements.[10−14] These isomers whose symmetry groups are given in parentheses (Schönflies notations) are T_4 (T_d)-$5^04^03^3$, T_6 (D_{3h})-$5^04^33^2$, T_8 (O_h)-5^04^6 and (C_{2v})-$5^24^23^2$, T_{10} (D_{5h})-$6^05^24^5$, T_{12} (D_{2d})-$6^05^44^4$ and (D_{6h})-$6^25^04,^6$ T_{14} (D_{3h})-$6^05^64^3$, (D_{3h})-$6^35^04^6$, and (C_{2v})-$6^15^44^4$, and T_{16} (D_{4d})-$6^05^84^2$, (D_{2d})-$6^45^04^6$, and (C_{3v})-$6^15^64^3$. This choice of isomers allows us to see the effect of different faces and edges of a given T cage, as well as of their sizes, on the structural and electronic properties of silsesquioxane.

3. Results and Discussion

3.1. Structural Properties. Tables 1 and 2 collect total energies and structural parameters which describe bond lengths and bond angles for various T cages at their optimized geometry on the LDA and NLDA levels of theory. Due to the presence of rings with different sizes in the same T cage, we classify the structural parameters on the basis of the rings which form an edge and do not give their average values over all rings. We use the notation of NR/N'R to represent the edge formed by an N-member and an N'-member ring. In Table 2, for example, the structural parameters of 3R/4R represent the values associated with atoms shared by three- and four-member rings.

In the connectivity scheme used here, the T_4, T_6, and T_{10} cages may only be represented by a single configuration whereas the T_8, T_{12}, T_{14}, and T_{16} cages may have a few isomeric configurations consisting of four-, five-, and six-member rings. According to Table 1, at the NLDA level, the lowest energy configurations for T_{12} and T_{14} correspond to the 5^b4^c unit whereas the T_{16} cage prefers the 6^a4^c unit. The NLDA results therefore reproduce successfully experimental observations[2−4] about the synthesis of pure T_{12} (D_{2d})-5^44^4 and T_{14} (D_{3h})-5^64^3 compounds. Furthermore, for the T_{14} cage, a second isomer with the C_{2v} symmetry is also possible since calculations find a small energy difference between the D_{3h} and C_{2v} configurations. In fact, X-ray diffraction experiments[4] have identified the structure of the second isomer to be C_{2v}. In the case of the T_{16} cage, the major isomer is suggested to be D_{4d}-$6^05^84^2$ on the basis of the observed[3] linear correlation between the number of four-member rings and ^{29}Si NMR chemical shifts. However, the NLDA results suggest D_{2d}-$6^45^04^6$ to be the major isomer. Although the LDA calculations find C_{3v}-$6^15^64^3$ to be the most stable isomer, both synthesis experiments and NLDA calculations do not find this to be the case for T_{16}. We conclude therefore that the NLDA level of theory we used is more appropriate for determining major isomers of higher silsesquioxane cages.

Analysis of total energies of various isomers of the T cages also reveals a progression of the preferred building unit with the increase in cage size. The preference for the four-member rings can be seen for T_8 while T_{12} prefers 5^44^4 over 6^24^6. For T_{14}, a combination of either five- and four-member rings or six-, five-, and four-member rings is preferred. On the other hand, the preference for 6^44^6 over 5^84^2 or $6^15^64^3$ is clearly shown in Table 1 for the T_{16} cage.

Comparison of LDA and NLDA structural parameters given in Table 2 shows a small increase in R_{Si-O} and A_{OSiO} in NLDA while A_{SiOSi} generally appears to become smaller in NLDA. For all of the T cages considered, the increase in the cage size has no effect on the bond lengths R_{Si-H} and R_{Si-O} but does have a noticeable effect on the bond angle A_{SiOSi}. This is expected due to a large variability of the bond angle which opens to accommodate more atoms as one goes from T_4 to T_{16}. This variability is clearly demonstrated by the results which show a comparatively large range of 140−159° for A_{SiOSi} as compared to the range of 110−112° for A_{OSiO}, respectively (Table 1—cf. T_{14} (C_{2v})).

A direct comparison of the calculated bond lengths and bond angles with X-ray diffraction data is not possible since calculations were performed for isolated molecules while the experimental data were obtained with single crystals. The molecular packing of silsesquioxanes in the crystal is expected to modify mainly A_{SiOSi} due to spatial constraints imposed by the crystalline state, leaving both R_{Si-O} and A_{OSiO} the same as in isolated molecules. For example, the calculated (NLDA) angular spread in A_{SiOSi} is 137−148° as compared to the range of 143−164° for the measured angle[14] of T_{12} (D_{2d}). On the other hand, both R_{Si-O} and A_{OSiO} are similar in molecular and crystal form with respective values of 168 pm, 109−111° and 162 pm, 108−111°. Both X-ray diffraction data on crystals, and the calculated results for molecules therefore suggest that silsesquioxanes can be described in terms of a network of rigid $HSiO_3$ cages where flexible Si−O−Si angles provide the molecular connectivity.

Looking at the ring-size dependence of the structural parameters, we find a large variation in R_{Si-O}, A_{SiOSi}, and A_{OSiO} in going from a three-member ring (T_4) to a four-member ring (T_8) which is in agreement with earlier theoretical[23] and experimental[25] studies. Thereafter, both R_{Si-O} and A_{OSiO} show a very small variation in going from a four-member ring to a six-member ring as compared to the variation in A_{SiOSi}.

Comparison of results obtained in the present study using density functional theory with previous calculations based on the Hartree−Fock (HF) approximation[23] shows well-known differences in the structural parameters arising from the use of two different methodologies. For the T_4 cage, R_{Si-O} and R_{Si-H} are reported to be 165.5 and 145.4 pm, respectively, in the HF study as compared to our NLDA values of 171 and 147 pm. The HF calculation for the T_{12} (D_{6h}) cage gives these bond lengths as 163 and 146 pm in contrast to our NLDA values of

TABLE 3: Binding Energies and Energies of the Hydrolysis Reaction for Various Configurations of Silsesquioxanes

	building unit	sym	binding energy/ Si atom (hartree)		energy of the hydrolysis reaction/ Si atom (kcal/mol)		
			LDA	NLDA	LDA	NLDA	HF[23]
T_4	$5^0 4^0 3^4$	T_d	−0.7139	−0.6021	−5.0	−5.7	−4.1
T_6	$5^0 4^3 3^2$	D_{3h}	−0.7234	−0.6117	+1.0	+0.3	+3.4
T_8	$6^0 5^0 4^6$	O_h	−0.7251	−0.6137	+2.1	+1.6	+5.9
	$5^2 4^2 3^2$	C_{2v}	−0.7246	−0.6127	+1.7	+1.0	+4.8
T_{10}	$6^0 5^2 4^5$	D_{5h}	−0.7249	−0.6134	+1.9	+1.4	+6.2
T_{12}	$6^2 5^0 4^6$	D_{6h}	−0.7247	−0.6131	+1.8	+1.2	+6.2
	$6^0 5^4 4^4$	D_{2d}	−0.7255	−0.6133	+2.3	+1.4	+6.4
T_{14}	$6^0 5^6 4^3$	D_{3h}	−0.7253	−0.6137	+2.2	+1.6	
	$6^1 5^4 4^4$	C_{2v}	−0.7257	−0.6136	+2.5	+1.5	
	$6^3 5^0 4^6$	D_{3h}	−0.6935	−0.5727	−17.8	−24.1	
T_{16}	$6^0 5^8 4^2$	D_{4d}	−0.7238	−0.6127	+1.2	+1.0	
	$6^1 5^6 4^3$	C_{3v}	−0.7252	−0.6118	+2.1	+0.4	
	$6^4 5^0 4^6$	D_{2d}	−0.7250	−0.6140	+2.0	+1.8	

167 and 147 pm. A similar variation can be found for the bond angles. The HF study reports A_{OSiO} as 105° in T_4 and 110° in T_{12} (D_{6h}) while the NLDA calculation gives 107° for T_4 and 113° for T_{12} (D_{6h}). In the T_4 and T_{12} (D_{6h}) cages, the respective values of A_{SiOSi} are 118 and 150° with HF and 114 and 163° using NLDA. Overall, the HF and NLDA values for R_{Si-O} and A_{OSiO} are within 3% of each other while they are within 10% of each other for A_{SiOSi}.

Table 1 also gives the energies obtained for the various cages and isomers relative to the value determined for T_4, so that the comparison of the LDA and NLDA with the HF energies can be more easily made. In Table 1, the values are in terms of the total energy per Si atom in units of kcal/mol. Note that the HF calculations place various T cages lower in energy than either LDA or NLDA calculations while the calculated stability of isomeric configurations is predicted to be the same by these methodologies. For T_8 and T_{12}, the most stable configurations have O_h and D_{2d} symmetries, respectively, in agreement with experiments.

3.2. Stability. Silsesquioxanes are unstable in the presence of hydroxyl groups and can undergo hydrolysis by the following reaction:[23]

$$(HSiO_{3/2})_n + (3/2)nH_2O = nHSi(OH)_3 \qquad (1)$$

The energetics of this reaction are expected to depend on the binding energy for a particular cage configuration and on the different fragmentation paths taken. Table 3 shows these energies per Si atom for the cages for which Table 1 lists the total energies. It is seen that this hydrolysis reaction is an endothermic process except for the T_4 cage. This is consistent with experimental observations and previously published theoretical calculations. The NLDA calculations find the energy of the hydrolysis reaction per Si atom in the range 0.3−1.8 kcal/mol, indicating that the isomeric configurations considered are relatively stable. We note here that the HF calculations[23] yield considerably higher values (in the range 3.4−6.4 kcal/mol) for this reaction energy.

The binding energy with respect to atomic constituents increases from T_4 to T_8, as expected, and then remains essentially constant, independent of the cage size, for both LDA and NLDA levels of theory, having values of 0.72 and 0.61

TABLE 4: Fragmentation Energetics of Silsesquioxanes Calculated Using Total Energies of the Optimized Configurations

fragmentation path	fragmentation energy (kcal/mol)	
	LDA	NLDA
$T_8 \rightarrow T_4 + T_4$	56.4	58.0
$T_{10} \rightarrow T_6 + T_4$	32.9	35.1
$T_{12} \rightarrow T_4 + T_4 + T_4$	87.7	84.4
$\rightarrow T_8 + T_4$	31.3	26.4
$\rightarrow T_6 + T_6$	15.9	12.5
$T_{14} \rightarrow T_6 + T_4 + T_4$	68.2	66.0
$\rightarrow T_{10} + T_4$	35.3	30.9
$\rightarrow T_8 + T_6$	11.8	8.0
$T_{16} \rightarrow T_8 + T_4 + T_4$	57.5	61.6
$\rightarrow T_6 + T_6 + T_4$	42.0	47.7
$\rightarrow T_{12} + T_4$	26.2	35.2
$\rightarrow T_{10} + T_6$	9.1	12.6
$\rightarrow T_8 + T_8$	1.1	3.6

TABLE 5: Compositions of HOMO and LUMO States in the (NLDA) Optimized Configurations of Silsesquioxanes in Terms of Percentage of Total Population

	HOMO				LUMO			
	state	Si	O	H	state	Si	O	H
T_4 (T_d)	T_1	0.3	1.7	0	E	0.94	0.43	0.63
T_6 (D_{3h})	E′	0.15	1.85	0	A_1'	0.24	0.61	0.15
T_8 (O_h)	A_{2g}	0	1.0	0	A_{1g}	0.3	0.54	0.16
T_{10} (D_{5h})	E_2'	0.1	1.9	0	A_1'	0.25	0.41	0.34
T_{12} (D_{2d})	E	0.1	1.9	0	A_1	0.21	0.37	0.42
T_{14} (D_{3h})	A_1''	0.03	0.97	0	A_2''	0.16	0.02	0.82
T_{16} (D_{2d})	B_2	0.03	0.97	0	E	0.33	0.02	1.65

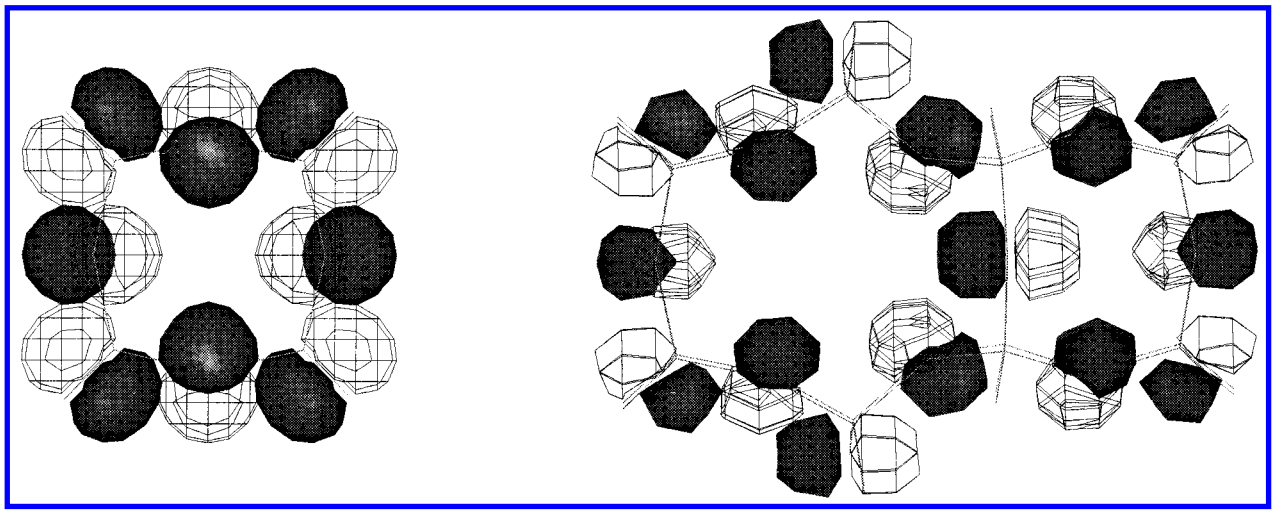

Figure 3. HOMO contours: (left) T_8 (O_h); (right) T_{16} (D_{2d}). Negative (dark solid contours) and positive (lines) regions are plotted with contours of 0.02 e/bohr^3.

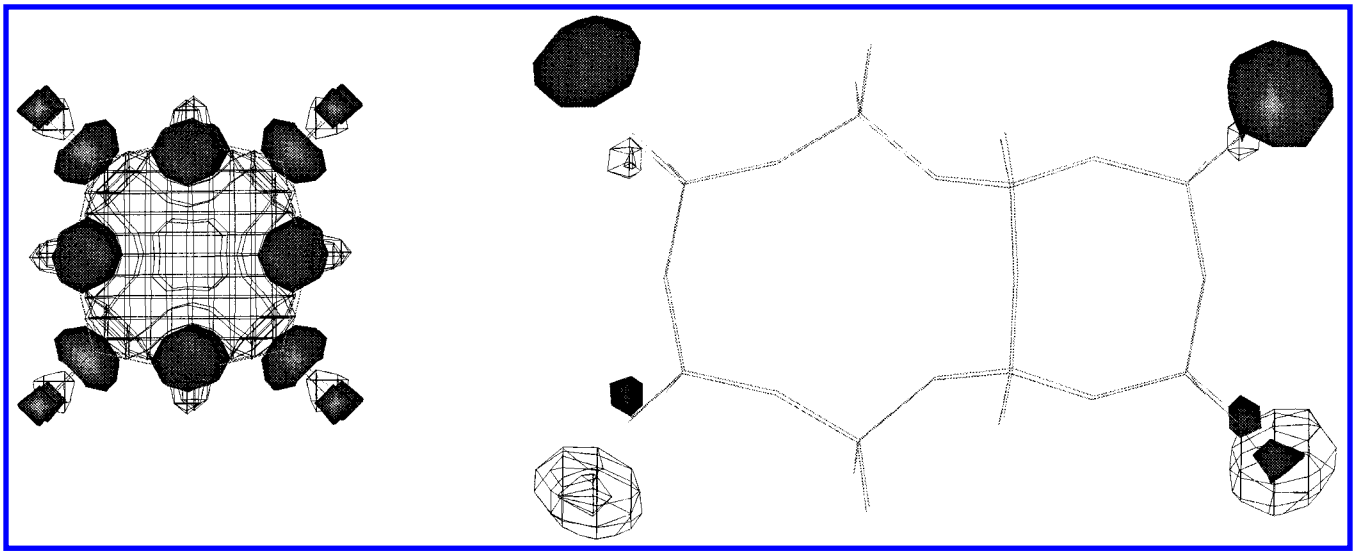

Figure 4. LUMO contours: (left) T_8 (O_h); (right) T_{16} (D_{2d}). Negative (dark solid contours) and positive (lines) regions are plotted with contours of 0.028 e/bohr^3.

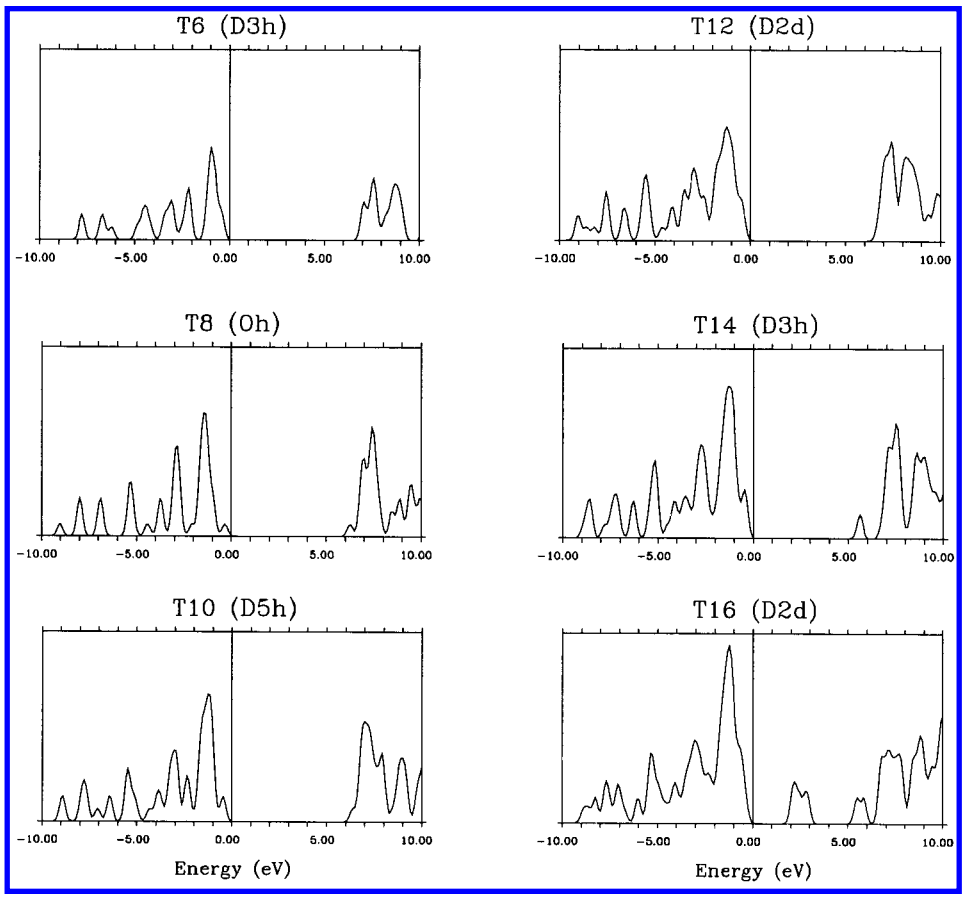

Figure 5. Total density of states plots for the optimized configurations of the T cages considered.

hartree per Si atom, respectively. Due to small differences in binding energies, the calculated results predict that various isomers of a given T cage can coexist, as is also observed in synthesis experiments.[2,3]

Calculations of the fragmentation energies with regard to all possible pathways support the above results in terms of the relative stability of the T cages considered in this study. Table 4 gives the fragmentation energies computed using the total energy of the most stable configurations. The dissociation of the T_{16} cage into two T_8 cages appears to have the lowest fragmentation energy followed by the dissociation of the T_{14} cage. On the other hand, T_8, T_{10}, and T_{12} cages appear to be the most stable against fragmentation into smaller T cages.

3.3. Electronic Properties. In this section, we present the results of the analysis of electronic properties of T cages in terms of density of states (DOS), deformation charge densities, highest occupied molecular orbitals (HOMOs), lowest unoccupied molecular orbitals (LUMOs), and Mulliken populations.

The spatial extents of the HOMOs and LUMOs for T_8 (O_h) and T_{16} (D_{2d}) are shown in Figures 3 and 4. The (lone-pair) oxygen p-type atomic orbitals form HOMOs in both T_8 and T_{16} (Figure 3) while a combination of atomic orbitals associated

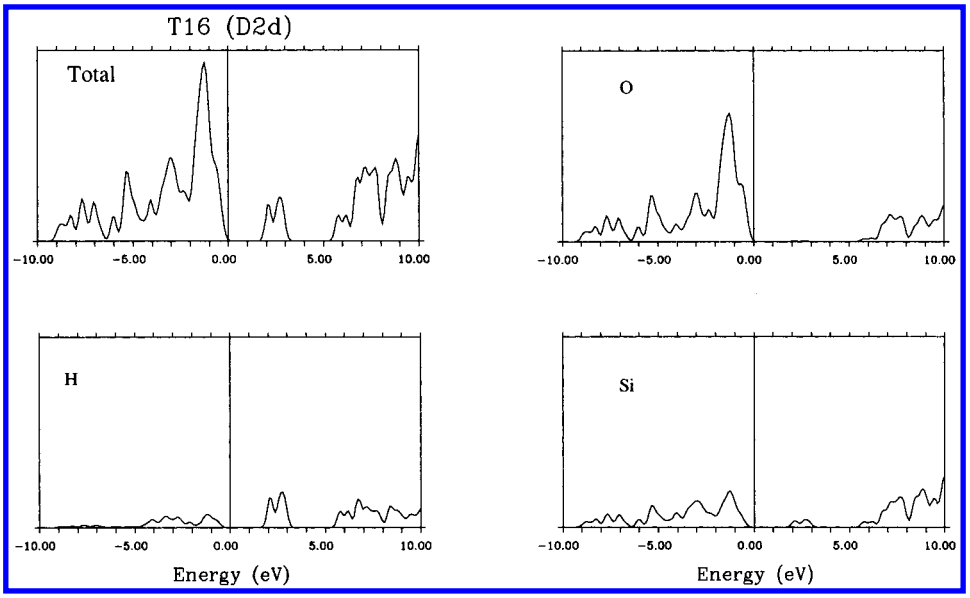

Figure 6. Projected density of states plots for T_{16}.

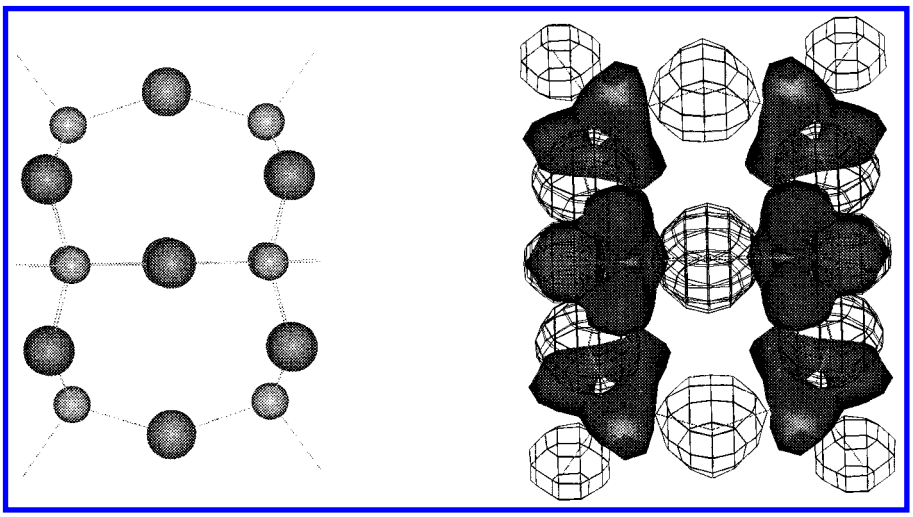

Figure 7. Deformation electronic density maps for T_8 (O_h). Negative (lines) and positive (dark solid contours) regions represent zones of surplus and lack of electronic density respectively and are plotted with contours of 0.01 e/bohr^3. In the accompanied ball-and-stick representation of T_8, the smaller circles represent silicons and the larger circles represent oxygens. The hydrogen atoms, not shown in the figure, are attached to silicons.

with Si, O, and H forms the LUMO for T_8. Interestingly, the percentage of the oxygen orbital mixing with the silicon and hydrogen orbitals for the LUMO decreases with the increase in the cage size, and in the case of T_{16}, the LUMO is marked by a negligible presence of oxygen orbitals (Figure 4). This is confirmed by Table 5, which shows the composition of the HOMO and LUMO orbitals for the most stable configurations of various T cages.

Density of states (DOS) for silsesquioxanes was analyzed using a Gaussian broadening scheme with a value of 0.15 eV, which was used to widen the discrete peaks of the T cages. Figure 5 compares the DOS plots for the T cages considered here where we have assigned the top of the occupied state to zero. As expected from the nature of the HOMOs, the highest occupied state is formed solely by the oxygen p lone-pair nonbonding orbitals. The O s orbitals are well separated from the O p orbitals and occur about 17 eV below the top of the occupied states. Adjacent to the highest occupied state, the DOS plots show a clustering of states up to about 9 eV wide below the top which is mainly due to bonding orbitals of silicon s-type and oxygen p-type orbitals.

The HOMO−LUMO gap shows a small variation with the cage size decreasing from 7.4 eV in T_6 to 6.2 eV in T_{16}. In the absence of experimental values of the gap for T cages, we can only make comparison of the calculated gap values with the known value[26] of about 9 eV for α-quartz. Note that calculations based on density function theory are known to underestimate the actual energy gap. A previous electronic structure calculation based on the extended-Hückel approximation[27] has reported the HOMO−LUMO gap to be of the order of 12−14 eV for the T_8 cage, which is too large a value for silica.

The DOS plots for the series of different silsesquioxane cages given in Figures 5 and 6 reveal that for the largest one analyzed, the T_{16} cage, the LUMO introduces a state in the HOMO−LUMO gap. The projection of the total DOS to constituent atoms of the T_{16} cage finds this midgap state to be associated with the terminal hydrogens attached to silicons in the cage. The appearance of this state is remarkable in that it offers an explanation for the electrical bistability observed in the *jV* characteristics of metal−insulator−metal devices prepared from the HSQ resin thin films with changes in conduction over 3 orders of magnitude.[9] This finding also suggests that larger

size cages in H-silsesquioxane could affect the dielectric properties of such materials.

The contour plots of the deformation charge density illustrate the electronic distribution in the bond formation for T_8 in Figure 7. Here, regions of excess electron density are shown with line contours and regions deficient of electron density are mapped by dark solid contours. Accordingly, deviations in sphericity of the electronic clouds display the presence of polarization effects that arise due to the charge transfer from Si to O. Mulliken population analysis at the NLDA level of theory associates charges of +1.0e and −0.7e with Si and O atoms in these clusters, respectively, and does not show any dependence on the cluster size. This is to be expected since the nature of chemical bonding in silsesquioxanes is mainly determined by the building block, ($HSiO_{3/2}$), and is not influenced by an increase in its size.

4. Summary

In this work, H-silsesquioxane cages of various sizes and conformations are studied in the framework of density functional theory. We use the LDA and NLDA levels of theory and the numerical basis set for electronic structure calculations. Although the results are consistent in LDA and NLDA, the reliable prediction of the most stable isomer for larger T cages requires the use of the NLDA level of theory. The calculated total energies show a clear preference for four- and five-member rings by the smaller cages and for four- and six-member rings by the larger cages. A detailed analysis of binding energy, energy for the hydrolysis reaction, and fragmentation paths suggests the relative stability of T_8, T_{10}, and T_{12} cages. Both T_4 and T_6 cages which contain three-member rings are found to be relatively unstable against hydrolysis in accordance with the results of experiments and earlier Hartree−Fock calculations. The (lone-pair) oxygen p-type atomic orbitals form the HOMO of the T cages considered while the terminal hydrogens associated with silicons appear to give rise to an electronic state in the HOMO−LUMO gap for the larger T cages.

Acknowledgment. This project was financially supported by the Dow Corning Corp. K.-H.X. acknowledges the Michigan Technological University for a Graduate Research Fellowship.

References and Notes

(1) Calzaferri, G. *Tailor-made silicon oxygen compounds: from molecules to materials*; Corriu, R., Jutzi, P., Eds.; Braunschweig: Wiesbaden, Germany, 1996.

(2) Frye, C. L.; Collins, W. T. *J. Am. Chem. Soc.* **1990**, *92*, 5586.

(3) Agaskar, P. A.; Klemperer, W. G. *Inorg. Chim. Acta* **1995**, *229*, 335.

(4) Agaskar, P. A.; Day, V. W.; Klemperer, W. G. *J. Am. Chem. Soc.* **1987**, *109*, 5554.

(5) Marcolli, C.; Laine, P.; Buhler, R.; Calzaferri, G.; Tompkinson, J. *J. Phys. Chem. B* **1997**, *101*, 1171.

(6) Bornhauser, P.; Calzaferri, G. *J. Phys. Chem.* **1996**, *100*, 2035.

(7) Bartsch, M.; Bornhauser, P.; Calzaferri, G.; Imhof, R. *J. Phys. Chem.* **1994**, *98*, 2817.

(8) Chandra, G. *Mater. Res. Soc. Symp. Proc.* **1991**, *203*, 97.

(9) Pernisz, U. C. *Proc. Electroceramics* **1994**, *4*, 823.

(10) Larson, K. *Ark. Kemi* **1960**, *16*, 215.

(11) Burgy, H.; Calzaferri, G. *J. Chromatogr.* **1990**, *507*, 481.

(12) auf der Heyde, T. P. E.; Burgi, H.-B.; Burgy, H.; Tornroos, K. W. *Chimia* **1991**, *45*, 38.

(13) Tornroos, K. W. *Acta Crystallogr.* **1994**, *C50*, 1646.

(14) Tornroos, K. W.; Burgi, H.-B.; Calzaferri, G.; Burgy, H. *Acta Crystallogr.* **1995**, *B51*, 155.

(15) *DMol User Guide*, version 2.3.6; Molecular Simulations Inc.: San Diego, CA, 1996.

(16) Vosko, S. H.; Wilk, L.; Nusair, M. *Can. J. Phys.* **1980**, *58*, 1200.

(17) Becke, A. D. *Phys. Rev. A* **1988**, *38*, 3098.

(18) Rosen, A.; Ellis, D. E.; Adachi, H.; Averill, F. W. *J. Chem. Phys.* **1976**, *65*, 3629.

(19) Delley, B. *J. Chem. Phys.* **1990**, *92*, 508.

(20) Veliah, S.; Pandey, R.; Newsam, J.; Vessal, B. *Chem. Phys. Lett.* **1995**, *235*, 53.

(21) Veliah, S.; Xiang, K.; Pandey, R.; Recio, J. M.; Newsam, J. *J. Phys. Chem.* **1998**, *102*, 1126.

(22) Pasquarello, A.; Hybertsen, M. S.; Car, R. *Phys. Rev. B* **1996**, *54*, R2339.

(23) Earley, C. *J. Phys. Chem Soc.* **1994**, *98*, 8693.

(24) Hill, J.-R.; Sauer, J. *J. Phys. Chem.* **1994**, *98*, 1238.

(25) Oberhammer, H.; Zeil, W.; Fogarasi, G. *J. Mol. Struct.* **1973**, *18*, 309.

(26) DiStefano, T. H.; Eastman, D. E. *Solid State Commun.* **1971**, *9*, 2259.

(27) Calzaferri, G.; Hoffman, R. *J. Chem. Soc., Dalton Trans.* **1991**, 917.